

Noise generator of interfering signals for suppression information leakage signal generated by liquid crystal monitor screen

Vitalii Kataiev¹, Dmytro Yevhrafov¹, Vasyl Karpinets¹, Yurii Yaremchuk¹, Nataliia Kunanets²

¹Vinnitsia National Technical University, Khmelnytsky highway 95, Vinnitsia, 21000, Ukraine

²Lviv Polytechnic National University, S. Bandery str., 12, Lviv, 79000, Ukraine

Abstract

The processes of signal generation in display adapter of personal computer monitors are considered, and a spectral representation of the indirectly radiated signal for the final analysis time is found for a simplified (with two shades) static image. The comb structure of the linear path frequency response of a specialized intelligence tool, which is best able to receive side radiation signals generated by personal computer monitors, is substantiated. It was concluded that for high-quality signal interception by a specialized intelligence tool, it is necessary to estimate the synchronization periods of frames and columns of a display screen. The structure of a noise generator built as a source of digital white noise, a digital comb filter and an antenna, is substantiated. The transfer function of the digital filter was found and calculation of its parameters was carried out. An algorithm for processing digital white noise is presented to achieve effective suppression of the information leakage channel for liquid crystal structure monitor screens.

Keywords

Side electromagnetic radiation and pickup, specialized intelligence tool, liquid crystal structures, digital White Gaussian noise, digital filters

1. Introduction

For most computers, the occurrence of side electromagnetic fields is an undesirable result of their operation. One of the sources of such fields is the working displays of personal computer monitors (PCs) based on liquid crystal structures (LCS). They radiate radio waves in the frequency range from 15 kHz to 900 Mhz [1] and can be intercepted by specialized intelligence tools (see Fig. 1).

There is little information on the principles of building such tools. It is known that they consist of a receiver, synchronized pulse generators, and manually controlled oscillators [2], and in order to understand the principles of operation of such systems, the structure of signals sent to the PC monitor should be considered.

Let's look at the temporal pattern of one of the RGB signals using a screen with a resolution of 800×600 pixels. Red (R), green (G), and blue (B) signals are fed to the monitor over an interval of 31.77 μs, consisting of a line of pixels with a duration of 25.17 μs and a trailing flyback sync pulse with a duration of 6.6 μs (see Fig. 2). To ensure that pixels are displayed within the visible screen space, the horizontal sync signal uses negative pulses to mark the start and end of each line. This guarantees that

CMiGIN 2022: 2nd International Conference on Conflict Management in Global Information Networks, November 30, 2022, Kyiv, Ukraine
EMAIL: vkataiev@ukr.net (V. Kataiev); dyevgrafov@ukr.net (D. Yevhrafov); v.karpinets@gmail.com (V. Karpinets); yurevyar@gmail.com (Yu. Yaremchuk); nek.lviv@gmail.com (N. Kunanets)
ORCID: 0000-0002-7458-7807 (V. Kataiev); 0000-0001-9651-1558 (D. Yevhrafov); 0000-0001-8148-2002 (V. Karpinets); 0000-0002-6303-7703 (Yu. Yaremchuk); 0000-0003-3007-2462 (N. Kunanets)



© 2022 Copyright for this paper by its authors.
Use permitted under Creative Commons License Attribution 4.0 International (CC BY 4.0).
CEUR Workshop Proceedings (CEUR-WS.org)

the pixels are properly aligned between the left and right edges. The duration of the horizontal sync pulse is $3.77 \mu\text{s}$. The time lag between the last pixel in the line and the rising edge of the horizontal sync pulse is $0.94 \mu\text{s}$, and between the beginning of a new pixel line and the trailing edge of the synchronizing horizontal sync pulse is $1.89 \mu\text{s}$.

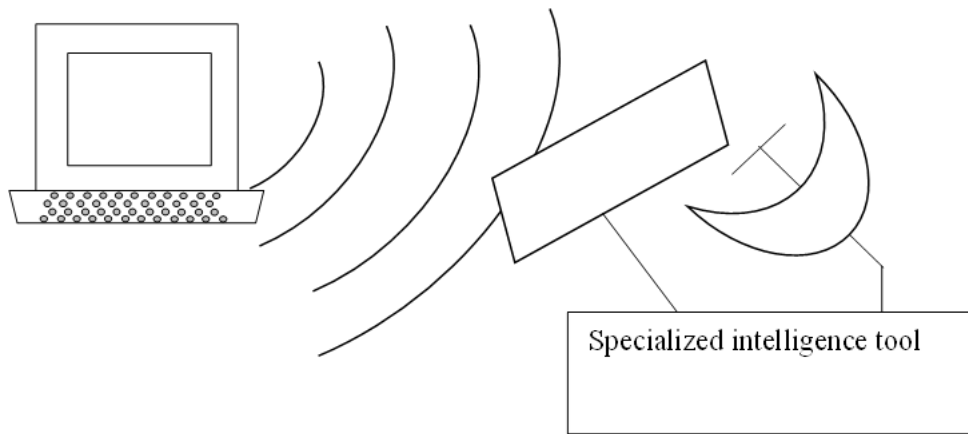


Figure 1: Information leakage radio channel of PC monitor screen

The monitor screen displays an image composed of three signals: red, green, and blue (RGB), which transmit color information to the monitor through a VGA cable. The intensity of each color component is determined by signal levels ranging from 0 V (complete darkness) to 0.7 V (maximum brightness), and when combined, create the color of a pixel on the screen.

The video frame on the monitor screen consists of h -lines of w pixels each, that is, it consists of $w \times h$ pixels with a standard resolution of 640×480 , 800×600 , 1024×768 and 1280×1024 . To create each frame, a pixel frame is sent to the monitor with the help of two synchronization signals. The first signal is horizontal and marks the beginning and end of each line of pixels that move from left to right on the screen. The second signal is vertical and marks the upper and lower lines that complete the frame.

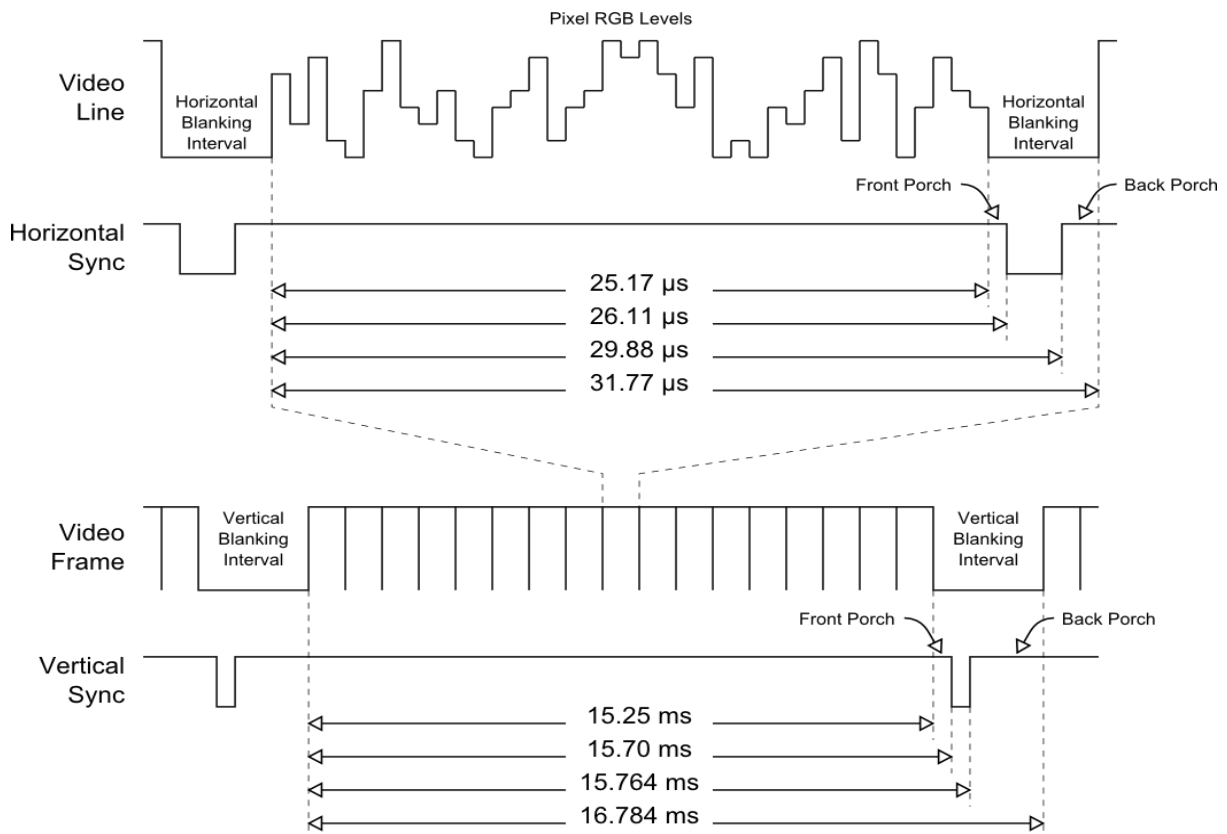


Figure 2: Display adapter R-G-B signals fed to the monitor

In the same way, pulses with a negative value on a vertical sync signal that lasts for 64 μ s indicate the start and end of a frame, guaranteeing that the lines displayed on the monitor are within the visible monitor space. At the same time, the time of each frame consists of the transmission time of all frames with a duration of 15.25 ms and the frame trailing flyback sync pulse with a duration of 1.534 ms, during which RGB signals are blocked. The time lag between the last frame line and the rising edge of the synchronizing vertical sync pulse is 0.45 ms, and between the beginning of the pixel line of a new frame and the trailing edge of the synchronizing horizontal sync pulse is 1.02 ms.

Problem statement: Substantiation of the signal spectrum of side electromagnetic radiation and pickup generated by PC LCS-based monitor screen displaying a static image of some meaningful, for example, text message. Let's consider the images to be sufficiently contrasting (for example, black letters on a white screen), that is, those having only two tones. In this case, multi-level R-G-B signals will have only two levels of amplitudes. LCS-based monitors have low radiation powers and large intervals of values for periods of synchronizing pulses.

Research objective: Substantiation of the noise generator structure preventing the operation of a specialized receiver for the side signals generated by LCS-based working monitor screen in the best way.

2. Active methods of information protection

Spatial noise involves the installation of a radio signal near the electronic equipment, which masks the signal in the place of its possible interception. The disadvantage of active protection of radio channels by noise generators is the impact on household radio equipment. After turning on the generator, all household radios, radios and some telephones start to "hiss" nearby, TVs "lower", images on computer monitors tremble. Although the level of radiation meets sanitary standards, radio waves near such a source do not add health to others.

Directional suppression is the formation with the help of an antenna system of sufficiently powerful high-frequency (RF) radiation, concentrated in some area. This allows not to create interference to the surrounding electronic equipment outside this area, and significantly reduces the need for scattering of large energy capacities.

When the receiver in this area of the receiver of the special means of reconnaissance in it is the RF signal modulated by the noise signal, and as a result of guidance and detection, the received signal will have a low-frequency noise component. Thus, in the suppression zone, along with the useful signal there is a much higher power-induced noise interference signal.

Noise generators "block" the radio channel of information leakage if they are placed near the receiver of the intelligence device. Since the location of the latter is unknown, the noise generator is placed near the source of information leakage. If the signal of the specialized intelligence tool is received in the band Δf_{np} , and the noise source has a spectrum width ΔF_3 , the information leakage channel is blocked if:

$$\frac{P_3 G_3}{\Delta F_3} \geq \frac{P_d G_d}{\Delta f_{np}},$$

where $G_3 \approx 1 - 3$, G_d – gain of antennas of noise generator and source of information leakage, P_3 , P_d – radiation power of noise generator and source of information leakage.

As a rule, generators produce noise signals with a Gaussian density of probability distribution of instantaneous values in the frequency range from 300 Hz to 7 MHz. Since the frequency range from 50 to 500 kHz is most often used to record information, it is in this range that the generator should emit the maximum level of spectral power density of the noise signal, and closer to the edges of the range the signal level should slowly fade. Most white noise generators operate in the upper frequency range from 10 MHz to 1200 MHz.

Many suppressors have a remote-control system that turns the generator on and off over the air and allows you to secretly turn it on and off when performing confidential work. Structurally, the suppressors are made in the form of separate blocks of the generator and antenna system, which allows

you to use them in both stationary and mobile versions (attachment case, suitcase, briefcase, etc.). There are camouflage options for a music center or personal computers.

3. Solving the problem

In [3], the frequency response of the linear part of a specialized intelligence tool receiver for a signal generated by the screens of CRT monitors is substantiated as follows:

$$|K(j\omega)| = \left| \frac{T_K \sin \left[\left(2 \operatorname{int} \left(\frac{T_a}{2T_K} \right) + 1 \right) \frac{\omega T_K}{2} \right] \sin \left(\frac{\omega T_a}{2} \right)}{2 \sin \left(\frac{\omega T_K}{2} \right) \omega} \right|, \quad (1)$$

where $\operatorname{int}(x)$ is a whole part of the x , T_K is a period of monitor vertical scan, and T_a is the time of analysis (accumulation) of information by a specialized intelligence tool. Frequency responses are of a comb nature. In Fig. 3 they are shown for $\frac{T_K}{T_a} = 20$, $\frac{T_a}{T_K} = 100$, $T_K = 1c$ and calculated according to (1).

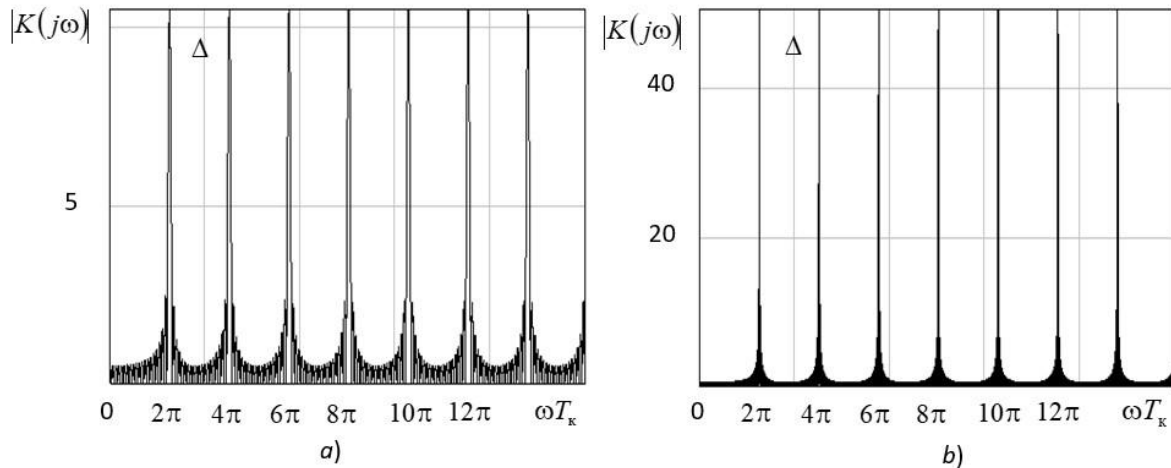


Figure 3: Frequency response of a specialized intelligence tool matched with the receiver signal: a) – $T_a/T_K=20$; b) – $T_a/T_K=100$

Since the signal intercepted by a specialized intelligence tool does not contain sync pulses, they are generated using column and frame scan generators to form an image. The required column pulses with frequency of $f_{hor} = 15 - 20kHz$ are fed from the column generator, and frame pulses with frequency of $f_{ver} = 40 - 80kHz$ are generated by dividing the frequency of column pulses according to the following expression:

$$f_{ver} = \frac{f_{hor}}{h}$$

where h is, as before, a number of lines on the CRT screen.

It is in the peaks of the combs with a frequency step of $\Delta = \frac{2\pi}{T_K} = 2\pi f_{ver}$ that the image generated by the monitor screen is "hidden", and other spectral components of the signal contain mostly meaningless information. Therefore, to fight side electromagnetic radiation and pickup in an active way, radiation in a wide frequency band will squander the energy of the noise generator into spectral components that do not contain any information. This applies especially to the information signal harmonics at relatively low frequencies. Thus, it is necessary to selectively suppress the spectral components of side electromagnetic radiation and pickup, which cannot be carried out by old-generation noise generators.

If the generator is built using modern digital filtering (DF) technology, in order to achieve maximum suppression of the side electromagnetic radiation and pickup signal, it is necessary that the noise signal spectrum is proportional to the frequency response of a specialized intelligence tool (1):

$$|K_{\phi}(j\omega)| \cong |K(j\omega)|, \quad (2)$$

where the synthesized filter gain is represented by the expression

$$K_{\phi}(j\omega) = \frac{a_n(j\omega)^n + a_{n-1}(j\omega)^{n-1} + \dots + a_1(j\omega) + a_0}{b_m(j\omega)^m + b_{m-1}(j\omega)^{m-1} + \dots + b_1(j\omega) + b_0}, \quad (3)$$

$a_0 - a_n, b_0 - b_m$ are some gains. A further problem of synthesis is to find the dependence of gains $a_0 - a_n, b_0 - b_m$ on the DF transfer function gains $A_0 - A_N, B_0 - B_M$:

$$H(z^{-1}) = \frac{Y(z^{-1})}{X(z^{-1})} = \frac{A_0 + A_1 z^{-1} + A_2 z^{-2} + \dots + A_N z^{-N}}{B_0 + B_1 z^{-1} + B_2 z^{-2} + \dots + B_M z^{-M}}, \quad (4)$$

where $Y(z)$ – is a conversion of the discrete response $y(kT)$ at the DF output, z is a conversion $X(z)$ of the discrete input effect $x(kT)$, k is a reference number of the signal samples, and T is the signal sampling interval.

Expression (4) is a transfer function of a linear discrete filter, but a real digital filter, unlike discrete filters, has nonlinear quantization effects in terms of rounding the results of operations. However, at the stage of approximation of characteristics, these effects can be ignored, and the DF can be considered as a linear discrete device with a transmission gain (3), which is obtained when the substitution $z = \exp(j\omega T) p = j\omega$ is made in (4):

$$K_{\phi}(j\omega) = \frac{A_0 + A_1 \exp(-j\omega T) + A_2 \exp(-2j\omega T) + \dots + A_N \exp(-Nj\omega T)}{B_0 + B_1 \exp(-j\omega T) + B_2 \exp(-2j\omega T) + \dots + B_M \exp(-Mj\omega T)}. \quad (5)$$

The modulus (5) is a periodic frequency response of the DF, and to find the gains $A_0 - A_N, B_0 - B_M$, the gains $a_0 - a_n, b_0 - b_m$ shall first be calculated during the transition from p -plane for (4):

$$K(p) = \frac{Y(p)}{X(p)} = \frac{a_n p^n + a_{n-1} p^{n-1} + \dots + a_1 p^1 + a_0}{b_m p^m + b_{m-1} p^{m-1} + \dots + b_1 p^1 + b_0},$$

$K(p)$ is a transfer function, $Y(p)$ is a Laplace Transform of response $y(t)$, $X(p)$ is a Laplace Transform of input effect $x(t)$, to z -plane. This problem is solved in [4] for the second-order bandpass filter transfer function:

$$H(z^{-1}) = \frac{A \cdot (1 - z^{-2})}{1 + A - Bz^{-1} + (1 - A)z^{-2}}, \quad (6)$$

in which the corresponding gains are related to the filter characteristics:

$$\omega_0 = \frac{1}{T} \arccos\left[\frac{B}{2}\right], \Delta\omega = \frac{2}{T} \arctg[A],$$

ω_0 is a central cyclic frequency of the filter, $\Delta\omega = 2\pi/T_a$ is a filter bypass band (cyclic frequency of the side electromagnetic radiation and pickup comb).

The DF can be considered as a linear discrete device with a transmission gain, which is obtained when the substitution $z = \exp(j\omega T) p = j\omega$ is made in (6):

$$K_{\phi}(j\omega) = \frac{A \cdot [1 - \exp(-2j\omega T)]}{1 + A - B \exp(-j\omega T) + (1 - A) \exp(-2j\omega T)}. \quad (7)$$

In Fig. 4 they are shown for $A = 0.01; 0.1, B = -2$ – dash-dotted line, $B = 0$ – dashed line, $B = 2$ – solid line, and calculated according to (7). In Fig. 5 they are shown for $A = 0.01; 0.1; 0.5, B = -1$ – solid line, $B = 1$ – dashed line, and calculated according to (7).

In order for the frequency response of the bandpass filter to be symmetrical with respect to each side electromagnetic radiation and pickup comb, $B = -2, B = 0$ and $B = 2$ at which $\omega_0 T = \pi, \omega_0 T = \pi/2$ and $\omega_0 T = 0$.

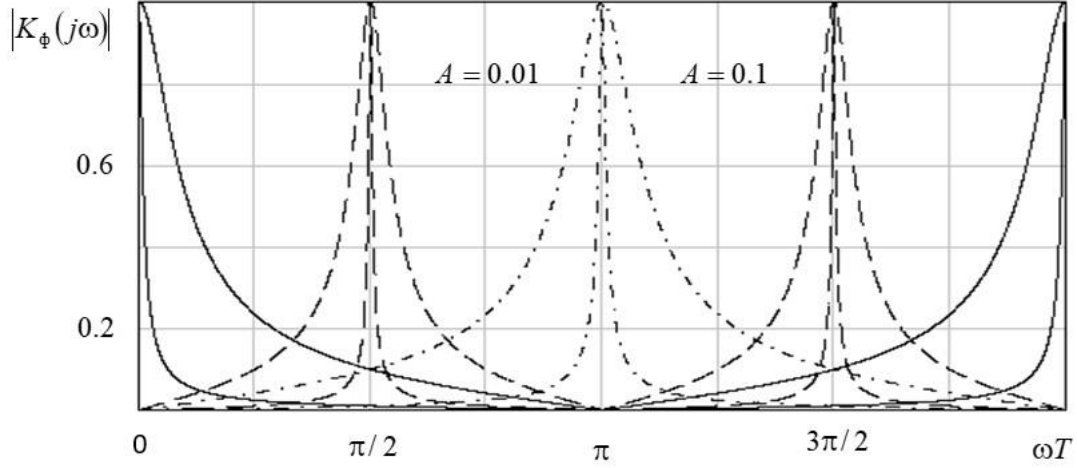


Figure 4: Normalized corresponding DF frequency responses (symmetrical)

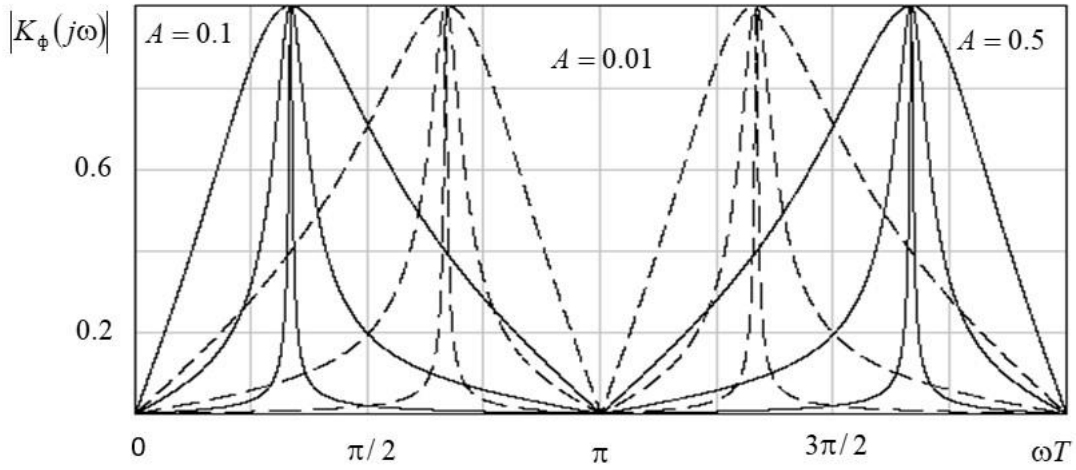


Figure 5: Normalized corresponding DF frequency responses (nonsymmetrical)

In Fig. 6 the dashed line indicates the individual side electromagnetic radiation and pickup comb calculated according to (1) for $\frac{T}{T_a} = 20$ and $\frac{T_a}{T} = 50$, and the solid line indicates the corresponding frequency response modules of the digital filters calculated for expression (7).

As can be seen, the resulting approximation allows to approach (1) quite correctly using the second-order DF.

4. M-combs generators

Expression (6) corresponds to the transfer function for generating a symmetrical single side electromagnetic radiation and pickup comb for $B = 2; -2; 0$. To generate M -combs, the sampling rate should be M times higher, and the DF transfer function should be as follows:

$$H(z^{-1}) = \frac{A \cdot (1 - z^{-2M})}{1 + A - Bz^{-M} + (1 - A)z^{-2M}} \quad (8)$$

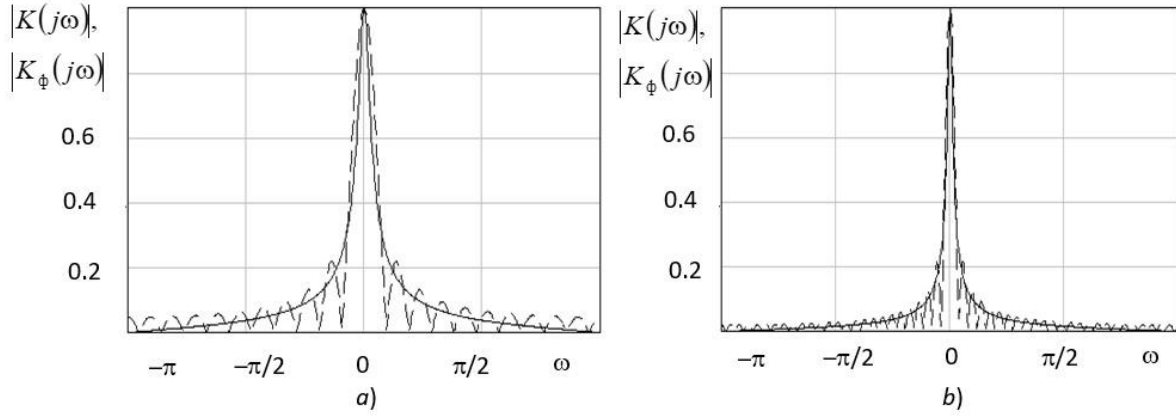


Figure 6: Normalized spectra of side electromagnetic radiation and pickup combs and corresponding DF frequency response: a) – $Ta/T=20$; b) – $Ta/T=50$

Thus, adding a digital filter with characteristic (7) to the White Gaussian noise (WGN) sample generator makes it possible to implement an adaptive noise generator (see Fig. 7), the efficiency of which is much higher than for broadband noise generators.



Figure 7: Block diagram of a noise generator

The implementation of the DF with the transfer characteristic (8) for $B = 2$ is shown in Fig. 8, where:

$$A^* = \frac{1-A}{1+A}, \text{ where } A = \text{tg}\left(\frac{\Delta\omega T}{2}\right) \quad (9)$$

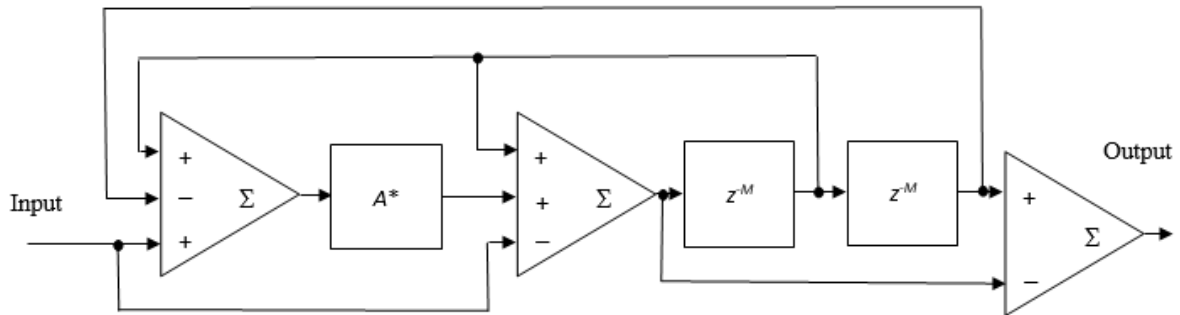


Figure 8: Implementation of the DF transfer function for $B=2$

The implementation of the DF with the transfer characteristic (8) for $B = -2$ is shown in Fig. 9, where A^* calculated for expression (9).

For the implementation of the DF transfer functions fig. 8 and fig. 9 the diagram contains shift registers for M -positions, the number of which can be estimated. For example, for a frame on a monitor screen consisting of 600 lines of 800 pixels each $f_{ver} = 75 \text{ Hz}$, but the side electromagnetic radiation and pickup spectrum has a maximum for frequencies of $f_{mid} = 350 \text{ MHz}$ and extends to approximately $f_{max} = 700 \text{ MHz}$ [5]. Subsequently, the generator will require a sampling rate of $1/T = 1.4 \text{ GHz}$, and $M = (f_{max} - f_{mid})/f_{ver} = 9333333$, which can be easily implemented using modern digital technologies.

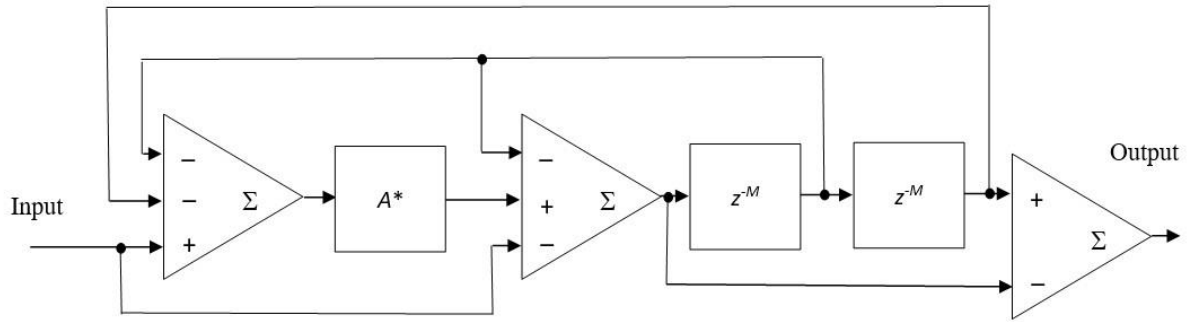


Figure 9: Implementation of the DF transfer function for $B=-2$

Expression (8) for $B = 0$ corresponds to the transfer function for generating a double side electromagnetic radiation and pickup comb (see a fig. 4). To generate M -combs, the sampling rate should be $4M/3$ higher, and the DF transfer function should be as follows

$$H(z^{-1}) = \frac{A \cdot (1 - z^{-2M})}{1 + A + (1 - A)z^{-2M}}, \quad (10)$$

end implementation of the DF with the transfer characteristic (10) is shown in Fig. 10, where A^* calculated for expression (9).

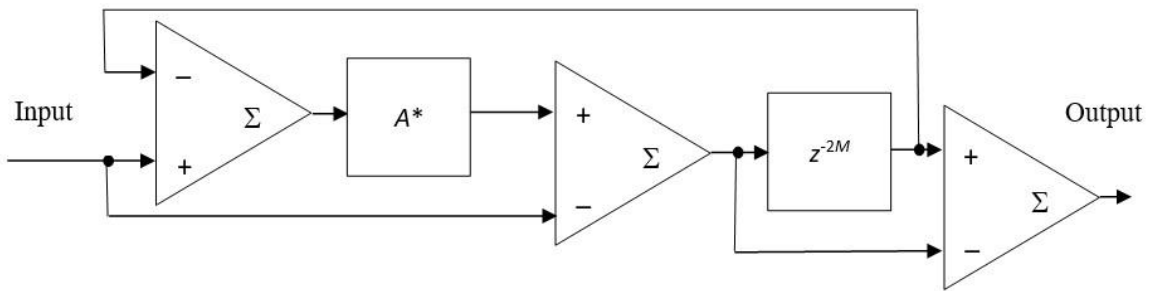


Figure 10: Implementation of the DF transfer function for $B=0$

Subsequently, the generator will require a sampling rate of $1/T = 4 \cdot f_{\max} / 3 = 933.33 \text{ MHz}$, and $M = (f_{\max} - f_{\text{mid}}) / 2f_{\text{ver}} = 4666667$, which more easily implemented.

5. Modeling of M-combs generator

Let's perform modeling in the program Matlab and Excel environment. For this purpose the digital array generated in the Matlab environment of $K=30000$ counts of white Gaussian noise (WGN) $n(t)$: $n_k = n(t)$, where $t = kT, k = 1, 2, \dots, K$, is passed via the digital filter described implementation of the DF transfer function for $B=2$ (see a Fig.8). The functional diagram of the experimental simulation is shown in Fig. 11, where M-combs filter, bandpass filter and fast Fourier transform is found in the program Excel environment [9-11].

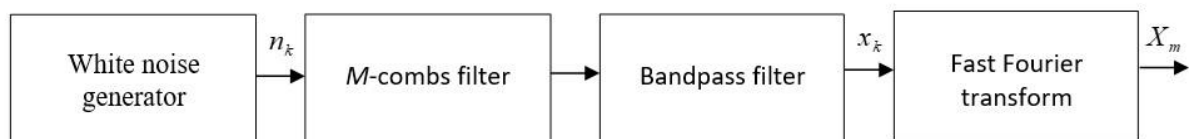


Figure 11: Functional diagram of experimental modeling

The bandpass filter "simulates" the selective properties of the radio propagation path and the broadband antenna system of the noise generator. Transfer function of bandpass filter is:

$$H(z^{-1}) = \frac{A \cdot (1 - z^{-2})}{1 + A + 2z^{-1} + (1 - A)z^{-2}}, \quad (11)$$

in which the corresponding gains are related to the filter characteristics:

$$f_{\text{mid}}T = 1/2, \text{ for } B = -2; A = \text{tg}[\pi(f_{\text{max}} - f_{\text{mid}})T/2].$$

Fast Fourier transform (FFT) K - time samples with a sampling interval T corresponds to the $N = K$ spectral components $f_n = n/TK$ $f_n = n/TK$ separated by frequencies on $1/TK$:

$$X_n = \sqrt{\left(\sum_{k=1}^K x_k \cos(2\pi nk / K)\right)^2 + \left(\sum_{k=1}^K x_k \sin(2\pi nk / K)\right)^2}, \quad n = 0, 1, \dots, N-1. \quad (12)$$

In Fig. 12 they are shown calculated according to (12) for this signal of the 100-combs generation.

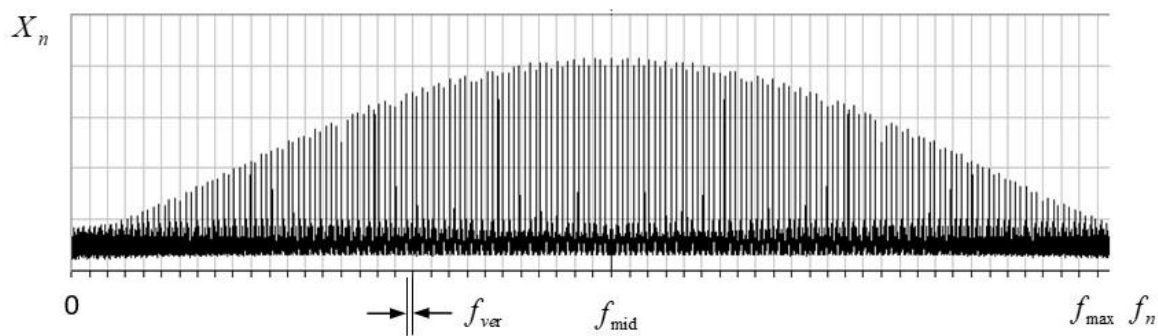


Figure 12: Spectrum of signal for the 100-combs generation

For this generator $M = \frac{f_{\text{max}} - f_{\text{min}}}{f_{\text{ver}}} = 100$.

6. Conclusions

The calculation expressions given in this work DF significantly simplify the assessment of the effectiveness of improving suppression generator for information leakage signal generated by liquid crystal monitor screen. Certainly, there is a certain distance from the theory to the specific DF, related to the acceptance or not of the simplifications that have been introduced. For example, frequency response M -combs filter and using the second-order DF. In practice, this is not the case. Nevertheless, a large number of results presented in the work, confirming the results of calculations by experimental modeling of generation processes, make the presented theory sound. The obtained results allow us to conclude that this method can be used for other channels of information leakage. Thus, the use of interfering counter-radiation in the infrared light range will provide protection against laser acoustic reconnaissance systems [6, 12, 13]. In this case, the probe's optical beam, by analogy with the hazardous signals from the monitor, will be masked by interfering signals that have parameters (eg, spectral, energy and space energy parameters) similar to dangerous signals. As a result, the process of removing the attacker's beam from many masking rays on the receiving part will be complicated.

7. References

- [1] Y. Kuznetsov, A. Baev, Methods for measuring side electromagnetic radiation and pickup: comparative analysis, *Confident 4-5* (2002) 54–57.

- [2] N. J. Gomes, P. P. Monteiro, A. Gameiro, Radio over Fiber Network Management, in: Next Generation Wireless Communications Using Radio over Fiber, Wiley, 2012, pp.247–263. doi: 10.1002/9781118306017.ch11.
- [3] D. Yevgrafov, Physical fundamentals of information protection in radio-electronic equipment: textbook, KPI, Kyiv, 2014, pp. 170–172.
- [4] H. L. Van Trees; K. L. Bell, Recursive Weiss Weinstein Lower Bounds for Discrete Time Nonlinear Filtering, in: Bayesian Bounds for Parameter Estimation and Nonlinear Filtering / Tracking, IEEE, 2007, pp.711–716. doi: 10.1109/9780470544198.ch71.
- [5] S. Arslan, B. S. Yıldırım, A Broadband Microwave Noise Generator Using Zener Diodes and a New Technique for Generating White Noise, Microwave and Wireless Components Letters 28(4) (2018) pp. 329–331. doi: 10.1109/LMWC.2018.2808422.
- [6] V. Kataiev, Y. Yaremchuk, UA Patent No. 137710 H01S 5/00. Kyiv: Method of creating active barriers to counteract unauthorized receipt of information by means of laser acoustic intelligence systems, u201902758; 11.11.2019, bul. № 21, 2019.
- [7] K. Bidaj, J. Begueret, J. Deroo, Generation of Colored Noise Patterns with Gaussian Jitter Distribution, IEEE Transactions on Instrumentation and Measurement 66(10) (2017) 2576–2584. doi: 10.1109/TIM.2017.2711738.
- [8] P. A. Traverso, C. Florian, F. Filicori, A Fully Nonlinear Compact Modeling Approach for High-Frequency Noise in Large-Signal Operated Microwave Electron Devices, Transactions on Microwave Theory and Techniques 63(2) (2015) 352–366. doi: 10.1109/TMTT.2014.2377737.
- [9] E. Napoli, G. Castellano, D. De Caro, D. Esposito, N. Petra, A. G. M. Strollo, Single Bit Filtering Circuit Implemented in a System for the Generation of Colored Noise, IEEE Transactions on Circuits and Systems I: Regular Papers 64(5) (2017) 1040–1050. doi: 10.1109/TCSI.2017.2656250.
- [10] J. Choi, J. Jung, I. Park, Area-Efficient Approach for Generating Quantized Gaussian Noise, IEEE Transactions on Circuits and Systems I: Regular Papers 63(7) (2016) 1005–1013. doi: 10.1109/TCSI.2016.2553318.
- [11] A. J. Uriz, P. D. Aguero, J. Moreira, R. M. Hidalgo, E. L. Gonzalez, J. C. Tulli, Flexible pseudorandom number generator for tinnitus treatment implemented on a dsPIC, Latin America Transactions 14(1) (2016) 72–77. doi: 10.1109/TLA.2016.7430063.
- [12] L. Weijun, C. He, X. Hao, An Active Cold and Hot Noise Generator, in: Proceedings of the International Conference on Microwave and Millimeter Wave Technology (ICMMT), 2019, pp. 1–3.
- [13] H. Ghanem, J. Gonçalves, P. Chevalier, I. Alaji, W. Aouimeur, S. Lepilliet, D. Gloria, C. Gaquière, F. Danneville, G. Ducournau, Modeling and Analysis of a Broadband Schottky Diode Noise Source Up To 325 GHz Based on 55-nm SiGe BiCMOS Technology, IEEE Transactions on Microwave Theory and Techniques 68(6) (2020) 2268–2277.